

Received: 2018.08.04

Accepted: 2018.10.12

Published: 2019.01.29

HIPK1 Interference Attenuates Inflammation and Oxidative Stress of Acute Lung Injury via Autophagy

Authors' Contribution:

Study Design A

Data Collection B

Statistical Analysis C

Data Interpretation D

Manuscript Preparation E

Literature Search F

Funds Collection G

BCD 1 **Lan Meng**

CDE 2 **Xin Zhao**

AF 2 **Hongxia Zhang**

1 Department of Anesthesiology, Qingdao Municipal Hospital of Shandong Province, Qingdao, Shandong, P.R. China

2 Department of Obstetrics, Qingdao Municipal Hospital of Shandong Province, Qingdao, Shandong, P.R. China

Corresponding Author: Hongxia Zhang, e-mail: qdzhanghx@163.com

Source of support: Departmental sources

Background: Acute respiratory distress syndrome (ARDS), which is characterized by severe hypoxemia ($\text{PaO}_2/\text{FIO}_2 \leq 300$ mmHg), is usually accompanied by uncontrolled inflammation, oxidative injury, and the damage to the alveolar-capillary barrier. Severe ARDS is usually accompanied with acute lung injury that worsen the patients' condition. HIPK1 is a modulator of homeodomain-containing transcription factors and regulates multiple cellular biological process associated with inflammation and anti-stress responses.

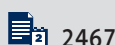
Material/Methods: We used an LPS-induced mouse acute lung injury (ALI) model to investigate the possible role of HIPK1 in ALI pathophysiology.

Results: We found the HIPK1 was elevated in ALI model mice while interference of HIPK1 by siRNA attenuated the inflammation and oxidative stress indicators (H_2O_2 , O_2^- , and NO). Further research found HIPK1 interference enhanced the autophagy.

Conclusions: Decreased HIPK1 in ALI showed protective effects in attenuating inflammation and oxidative stress and enhancing autophagy, indicating HIPK1 as a possible target in ALI management.

MeSH Keywords: **Acute Lung Injury • Autophagy • Inflammation**

Full-text PDF: <https://www.medscimonit.com/abstract/index/idArt/912507>



Background

Acute respiratory distress syndrome (ARDS), characterized by severe hypoxemia ($\text{PaO}_2/\text{FIO}_2 \leq 300$ mmHg) [1], is usually accompanied by uncontrolled inflammation, oxidative injury, and alveolar-capillary barrier damage. Acute lung injury (ALI) is a major pathogenesis of acute respiratory distress syndrome (ARDS), pneumonia, and acute respiratory failure (ARF) [2]. Previous studies have discovered that key pathological features of ALI – uncontrolled inflammation, oxidative injury, and damage to the alveolar-capillary barrier – resulted from apoptosis or inflammation [3]. The initial exudative phase of ALI is often triggered by the release of inflammatory cytokines and chemokines, which lead to the onset of damage [4–6]. Inflammation processes induced by the exposure to pathogen-associated molecular patterns (PAMPs) or danger (or damage)-associated molecular patterns (DAMPs) play important roles in onset of the overall process [2,4,7]. Investigating applicable methods to reduce the inflammation process and improve regional repair may provide indications for the clinical treatment of ALI.

Autophagy is a catabolic process that isolates proteins and organelles by double-membrane vesicles and is targeted to the lysosome for proteolytic degradation [8]. It has been reported that upregulation of autophagy attenuates the inflammation and improves survival by reducing organ dysfunction [8–11]. In contrast, inhibition of autophagy leads to exacerbated injury and increased mortality [8,9,11]. Thus, autophagy might be a promising target for the treatment of ALI.

Homeodomain-interacting protein kinase 1 (HIPK1) is a modulator of homeodomain-containing transcription factors [12,13]. Previous research has proposed HIPK1 as a pro-oncogenic gene that mediated apoptosis and DNA-damage repair [12,14,15]. It has important roles in cell stress and injuries in numerous diseases. HIPK1 can modulate p53 phosphorylation and leads to further p53 transactivation [12,16,17]. Other research also reported that inhibition of p53 leads to enhanced autophagy and thus ameliorates inflammation [17,18]. Therefore, we investigated the HIPK1 function in ALI and its protective effects through the regulation of autophagy.

Material and Methods

Animals

Eight-week-old C57 BL/6 male mice weighing about 22.1 g were used in the present study. These mice were bought from the Experimental Animal Centre of Qingdao University (Qingdao, China) and the study was approved by the Animal Care and Use Committee of Qingdao University (20170197-02) (Qingdao, China). They were placed in a specific pathogen free (SPF)

room with sawdust bedding at a temperature of 25–26°C and a relative humidity of ~50%, a 12-h light/dark cycle, and free access to water and food. We confirmed that all animals received human care and all animal experiments were conducted in accordance with the relevant guidelines and regulations.

LPS induction and HIPK1 interference

LPS induction was performed under anesthesia using the procedure described in a previously published study [19]. Bacterial LPS (0.63 mg/kg body wt; *Escherichia coli* O55: B5) or sterile water was injected intratracheally in a small volume (10–20 μl) via a 20-gauge catheter (Exelint International, Los Angeles, USA). Bafilomycin A (10 mg/kg) or chloroquine (CQ) (50 mg/kg) was administered 2 h prior to LPS induction. At 6, 12, and 24 h after LPS induction, lung tissues and blood were harvested in bafilomycin A treatment experiments, while in other experiments the mice were sacrificed and lung tissues and blood were harvested at 24 h for further analysis. The transfection procedure was applied as previously reported [20]. Briefly, the siRNA sequence of HIPK1 (Sense: 5'-GAGUAGCUGUGUUGUGUAA-3'; anti-sense: 5'-UUACACAACACAGCUACUC-3') or vector sequence were diluted with 10 μl of Opti-MEM and mixed gently; then, Lipofectamine™ 2000 (10 μl) was diluted with 20 μl of Opti-MEM, mixed gently, and incubated for 15 min at room temperature. The HIPK1 interference group received 30 μl mixed siRNA-lipofectamine intratracheally, while the vector group was treated with vector-lipofectamine for LPS induction.

Histology analysis

Lungs tissues were fixed in 4% paraformaldehyde solution for at least 2 days and then embedded in paraffin and sectioned. After deparaffinization and rehydration, the sections were stained with hematoxylin and eosin (HE). We used light microscopy to assess alveolar congestion, hemorrhage, aggregation of inflammatory cells, and the thickness of the alveolar barriers.

Analyses of H_2O_2 and $\text{O}^{\cdot-}$ production, and ROS levels in lung of mice

Lung levels of $\text{O}^{\cdot-}$ were measured using the chemiluminescence method. Firstly, the weighed lung tissues of mice were homogenized in lysis buffer, pH 7.4, containing 10 mM EDTA as well as 20 mM HEPES. The samples were centrifuged for 10 min at 1000 g, and then the aliquot of samples was incubated with a Krebs-HEPES buffer, pH 7.4, containing 5 mM lucigenin (Sigma, Shanghai, China) about 2 min at 37°C. Next, light emission data were obtained on a M200 PRO multifunctional microplate reader (TECAN, Switzerland), and the results were shown as mean light unit (MLU) min/mg protein. Levels of $\text{O}^{\cdot-}$ were measured by adding SOD (350 U/mL) to

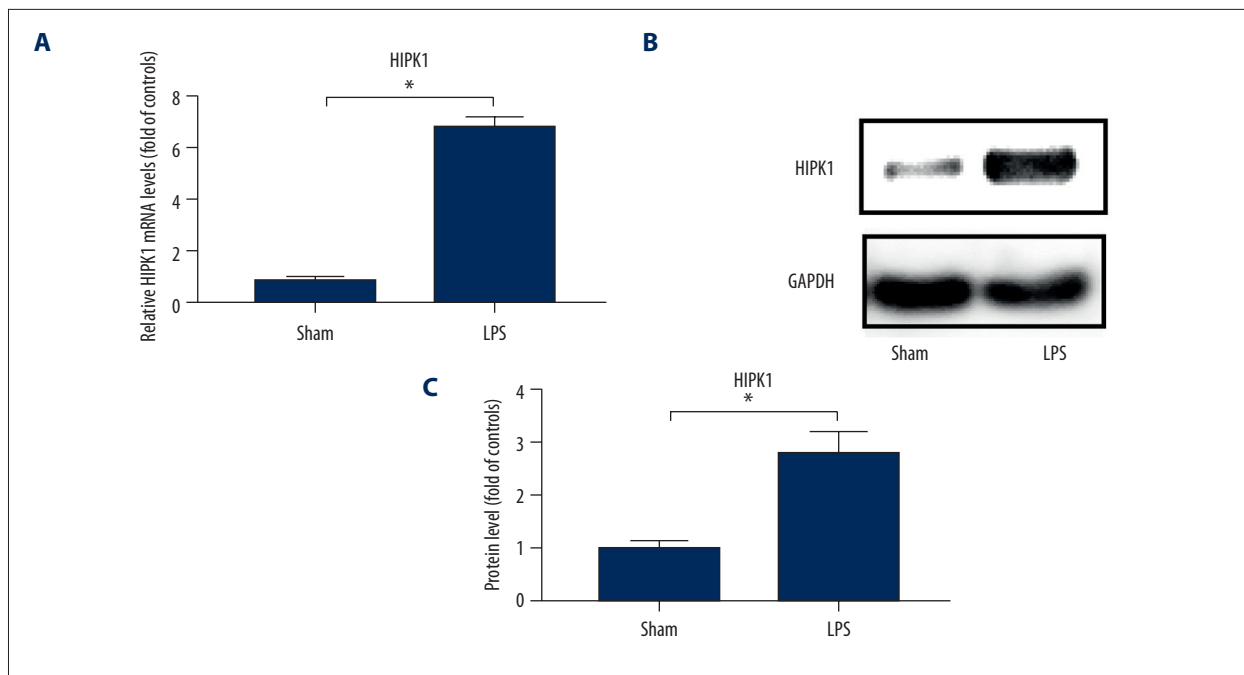


Figure 1. HIPK1 expression in LPS-induced acute lung injury. (A) mRNA level of lung tissue in LPS-induced ALI mice (LPS) and controls (sham). (B, C) Western blot (B) and quantification (C) of protein level of HIPK1 in LPS-induced ALI mice and controls. The data are presented as means \pm SEM (n=3), * p<0.05 compared with the sham group.

the medium according to the manufacturer instructions (R&D system, Minneapolis, MN, USA). Lung tissues were homogenized in normal saline, and the samples were treated with an equal volume of cold methanol for 60 min at 4°C. Then, the samples were centrifuged for 30 min at 10 000 g and we obtained the supernatant for H₂O₂ evaluation using biochemical kits (R&D Systems, Minneapolis, MN, USA). Protein concentration was measured using the Bradford method and BSA was employed as the standard.

Determination of TNF- α and IL-6 by ELISA

The weighed lung tissues were put in cold PBS buffer (pH 7.0) containing 0.002% sodium acid, 0.1 mg/mL soybean trypsin inhibitor, 2 mM PMSF, 10 nM EDTA, and 1.0 mg/mL BSA. The tissues were homogenated and samples were incubated for 2 h at 4°C. For further assays, the supernatants were collected by centrifugation at 12 000 g for 10 min. TNF- α , and IL-16 levels in supernatant of serum and lung were measured using ELISA kits (Sigma, Shanghai, China).

Reverse transcription-polymerase chain reaction (RT-PCR)

The reverse transcription-polymerase chain reaction (RT-PCR) and the quantitative real-time PCR (Q-PCR) were performed as follows. Total RNA was extracted from lung tissues and cultured cells using TRIZOL reagent (Thermo Fisher Scientific, Waltham, MA, USA). The cDNA was obtained by reverse transcription in

a 20- μ L reaction containing 2 μ g of total RNA, oligo (dT), and reverse transcription premix.

The quantitative real-time PCR (Q-PCR) reactions were performed with the SYBR green PCR system in an ABI 7500 thermal cycler (Thermo Fisher Scientific, Waltham, MA, USA). The SYBR green reagents were also purchased from Thermo Fisher Scientific. The cycling conditions were as follows: 95°C for 3 min; followed by 40 cycles involving denaturing at 95°C for 10 s, annealing at 60°C for 5 s, and extension at 72°C for 10 s. Expression of mRNAs was normalized by the mRNA levels of GAPDH, which was used as an internal control. We analyzed the relative levels of mRNAs using the 2^{- $\Delta\Delta$ Ct} method, and GAPDH was used as the internal control. The primer sequence was: HIPK1: forward, 5'-TCCCCTACTACGAGAGGGT-3'; reverse, 5'-ATGTCCCACCCCTAGTACC-3'; GAPDH: forward, 5'-CATTCAAGACCGGACAGAGG-3'; reverse, 5'-ACATACTGCAC ACCAGCATCACC -3'.

Immunoblot analysis

The lung tissues or the HSCs were lysed in RIPA Buffer (1 mM EDTA pH 8.0, 50 mM Tris-HCl pH 8.0, 2% SDS, 5 mM DTT), and their protein concentration was determined by BCA assay (Beyotime, Inc., Shanghai, China). The total protein (about 30 μ g) was separated by SDS-PAGE gel and transferred to PVDF (polyvinylidene fluoride) membranes (Invitrogen, California, USA), and blocked with 5% non-fat dry milk in

PBST (phosphate-buffered saline with Tween), pH 7.5. The membranes were immunoblotted with primary antibodies for 4 h or overnight at 4°C. The primary antibodies were all purchased from Cell Signaling Technology (Massachusetts, USA) and they were diluted at 1: 1000 in the immunoblot analysis. Secondary antibodies with horseradish peroxidase were used. The protein bands were assessed using an enhanced chemiluminescence kit (Pierce, Rockford, USA). The corresponding semi-quantitative analysis was based on optical density with ImageJ software.

Statistical analysis

Data are showed as the mean \pm SEM. The *t* test was performed for comparisons between 2 groups and one-way ANOVA was used for comparisons among more than 2 groups. *P* value <0.05 was considered to be statistically significant.

Results

HIPK1 expression in lung of LPS-induced ALI mice

We first analyzed HIPK1 expression in LPS-induced ALI mice. We found the HIPK1 was highly elevated in the lung tissue, as analyzed by Q-PCR (Figure 1A). Similarly, a low level of HIPK1 protein was found in lung tissue from LPS-induced ALI mice, as detected by Western blot analysis with quantification analysis (Figure 1B, 1C).

HIPK1 interference improved the pathology and attenuates regional inflammation and oxidative stress of lung tissue

We then used si-HIPK1 to interfere in the expression of HIPK1 in lung tissue by using Lipofectamine™ 2000. First, we proved that si-HIPK1 successfully downregulated the expression of HIPK1 at mRNA and protein levels in lung tissue (Figure 2A, 2B). We found that the interfered group showed ameliorated inflammation and pathological changes compared with the control vector of HIPK1 transfected group (con-HIPK1) and model group (Figure 2C). The cytokine level (IL-6 and TNF- α) in lung and peripheral blood were decreased in the si-HIPK1 group (Figure 2D–2G) and the pathology was improved according to HE staining (Figure 2C). In addition, as oxidative stress participates in the early phase of ALI and usually results in extensive inflammation, we next analyzed the level of H₂O₂, O⁻², and NO in the lung to determine the effects of HIPK1 on oxidative stress in LPS-induced mice. We found that H₂O₂, O⁻², and NO levels were elevated in LPS group, whereas si-HIPK1 inhibited H₂O₂, O⁻², and NO production in the lung of LPS-induced mice (Figure 3H–3J). These results indicated the protective effects in oxidative stress and inflammation in HIPK1-interfered mice.

HIPK1 interference enhanced autophagic flux in the lung of LPS-induced mice

In investigating possible mechanisms of HIPK1 interference in reducing inflammation and oxidative stress, we analyzed the level of LC3-II and p62 to investigate the possible alteration in autophagy. We found the expression of LC3-II and p62 was increased when compared with the control group (Figure 3A–3C) in LPS-induced lung tissue. After the interference of HIPK1, LC3-II further increased while p62 decreased compared with LPS-induced ALI mice (Figure 3A–3C). Bafilomycin A was used to detect the autophagic flux by inhibiting the degradation of the autophagosome. When treated with bafilomycin A in LPS-induced ALI mice, we found a significantly increase in LC3-II protein (Figure 3D, 3E). In addition, si-HIPK1 further enhanced LC3-II in the presence of bafilomycin A (Figure 3D, 3E). Thus, these results indicated the enhance autophagic flux of si-HIPK1 in LPS-induced ALI mice.

After discovering the effects of HIPK1 on autophagy in lung tissue, we next studied whether the autophagy is responsible for the ameliorated inflammation and oxidative stress of LPS-induced ALI. We used chloroquine (an autophagic flux inhibitor) to determine the contribution of autophagy in lung protection. We found that chloroquine increased the LC3-II expression (Figure 3F, 3G) and reversed the indicators of inflammation (IL-6 and TNF- α) (Figure 4A–4D) and oxidative stress (H₂O₂, O⁻², and NO) (Figure 4E–4G). Thus, these results proved the protective effects of autophagy in LPS-induced ALI and the regulatory role of HIPK1 in protecting lung tissue through autophagy.

HIPK1 interference restored the formation of autophagosomes and autolysosomes in LPS-induced ALI

The matured autophagosome is formed by Atg12-5 complex, Beclin-1 complex, and LC-3II. We detected the level of Atg12-5 protein by Western blot and found an elevation in LPS-induced ALI mice. After the HIPK1 interference, the Atg12-5 level was further enhanced (Figure 5A, 5B), while Beclin-1 showed no significant changes (Figure 5A, 5C). In addition, we also analyzed the level of LC3-lipidation by using Atg3 and Atg7 as markers. We found the Atg3 expression was reduced in LPS-induced ALI mice but was restored after HIPK1 interference, and Atg7 showed no significant changes (Figure 5A, 5D, 5E). These results proved that HIPK1 interference led to the restored level of autophagosome formation.

Discussion

Autophagy has been proved to be important in ameliorating sepsis-induced dysfunction of multiple organs. Previous research

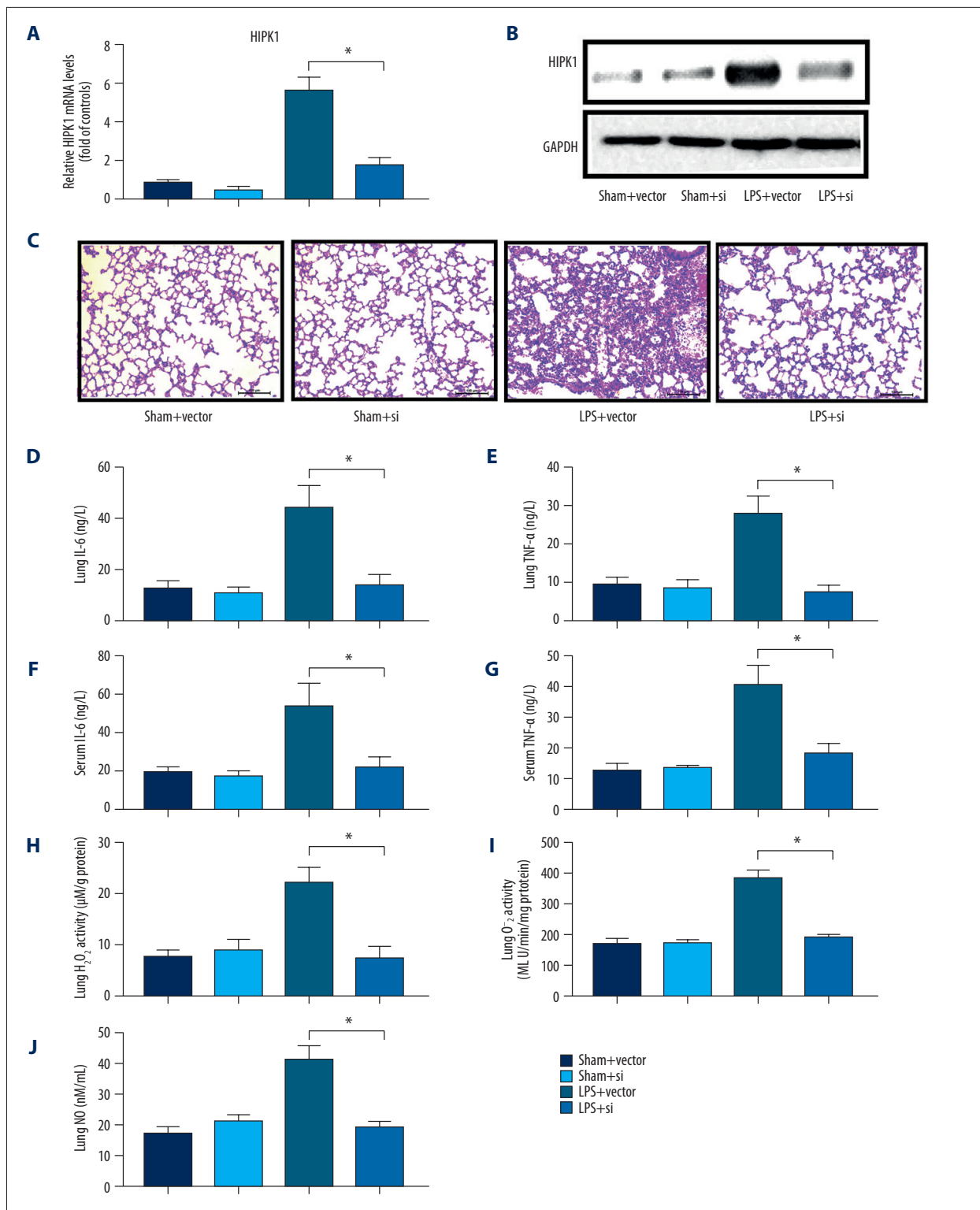


Figure 2. Ameliorated inflammation and injury of LPS-induced ALI mice after HIPK1 interference. **(A, B)** mRNA **(A)** and protein level **(B)** after HIPK1 interference in LPS-induced ALI mice. **(C)** HE staining of lung in LPS-induced ALI mice or sham mice after HIPK1 interference or vector. **(D–G)** IL-6 level in lung tissues **(D)** and serum **(F)**, and TNF-alpha in lung tissues **(E)** and serum **(G)** of different groups. **(H–J)** oxidative marker, H₂O₂ **(H)**, O⁻² **(I)**, and NO **(J)** in lung tissues of different groups. The data are presented as means \pm SEM (n=3), * p<0.05 compared with the sham group.

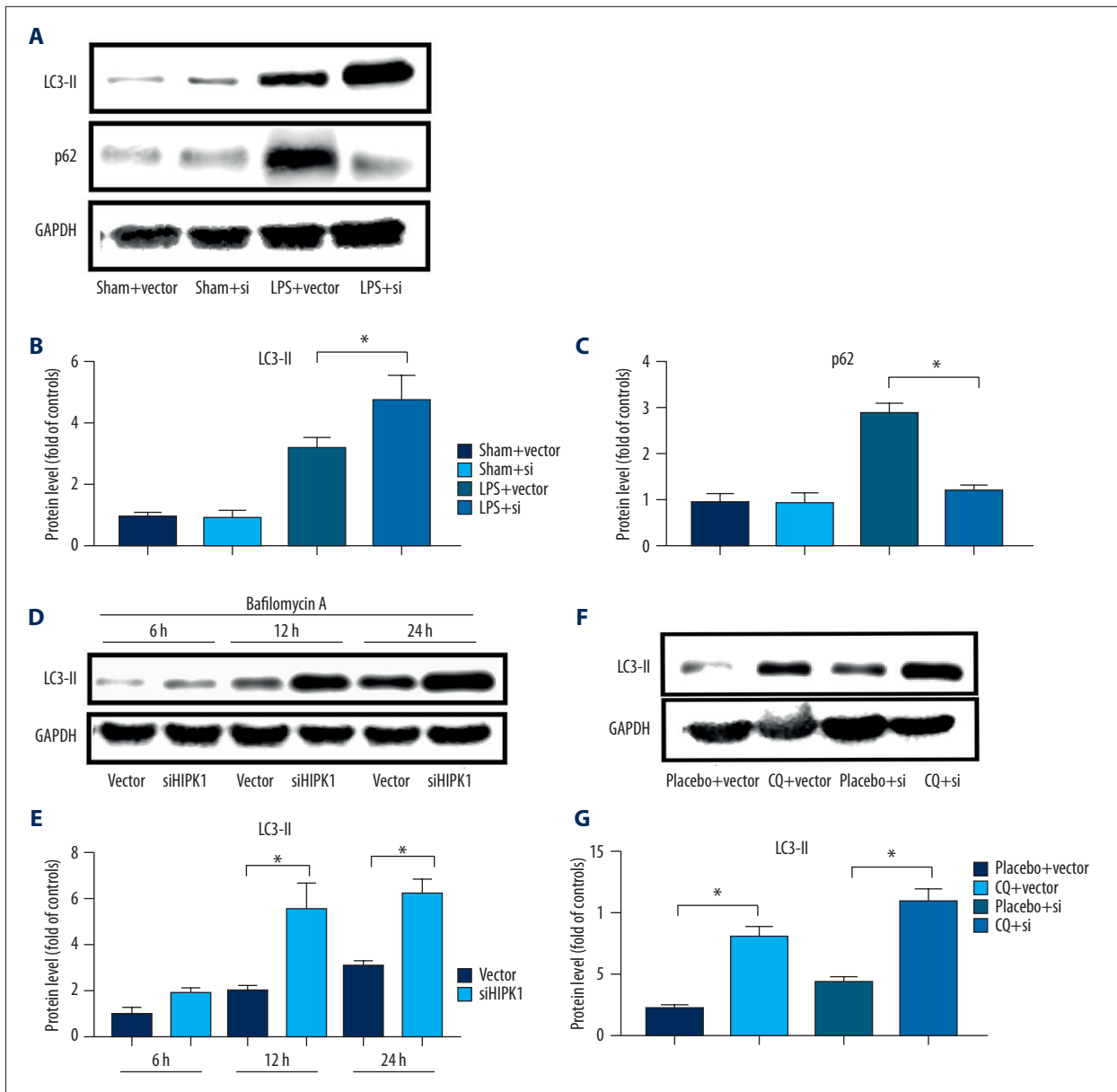


Figure 3. HIPK1 interference enhanced LC3-II expression and autophagic flux. (A–C) Western blot of LC3-II and p62 expression (A) and quantification (B, C) of lung in LPS-induced ALI mice or sham mice after HIPK1 interference or vector. (D, E) Western blot of LC3-II (D) and quantification (E) in lung tissue of vector or HIPK1 interference treated with bafilomycin A at different time points. (F, G) Western blot of LC3-II (F) and quantification (G) of LC3-II in lung tissue of vector or HIPK1 interference treated with chloroquine (CQ). The data are presented as means \pm SEM (n=3), * p<0.05 compared with the sham group.

found that inhibited autophagy led to increased mortality and morbidity through depleting immune cells and causing organ dysfunctions, whereas upregulated autophagy significantly attenuated organ injury. HIPK1 has been identified as one of the nuclear protein kinases participating in the regulation of several processes, including cell growth and apoptosis. Originally, HIPK1 was defined as a modulator of homeodomain-containing transcription factors [15]. However, recent research found comprehensive activity of HIPK1 in apoptosis [17], tumor

aggression [12], DNA-damage repair [13], and pro-oncogenic functions [12,13,16]. With in-depth understanding of HIPK1 in cancer research, recent studies discovered that HIPK1 interacts with p53 by phosphorylating serine-15 and thus promotes p53 transactivation [12,17]. However, the depletion, inhibition, or loss of p53 further enhances the autophagy and ameliorates cell stress in response to injuries [12,17], but it is unclear whether HIPK1 regulates autophagy in organ injury and dysfunctions. In this study, the HIPK1 interference in LPS-induced

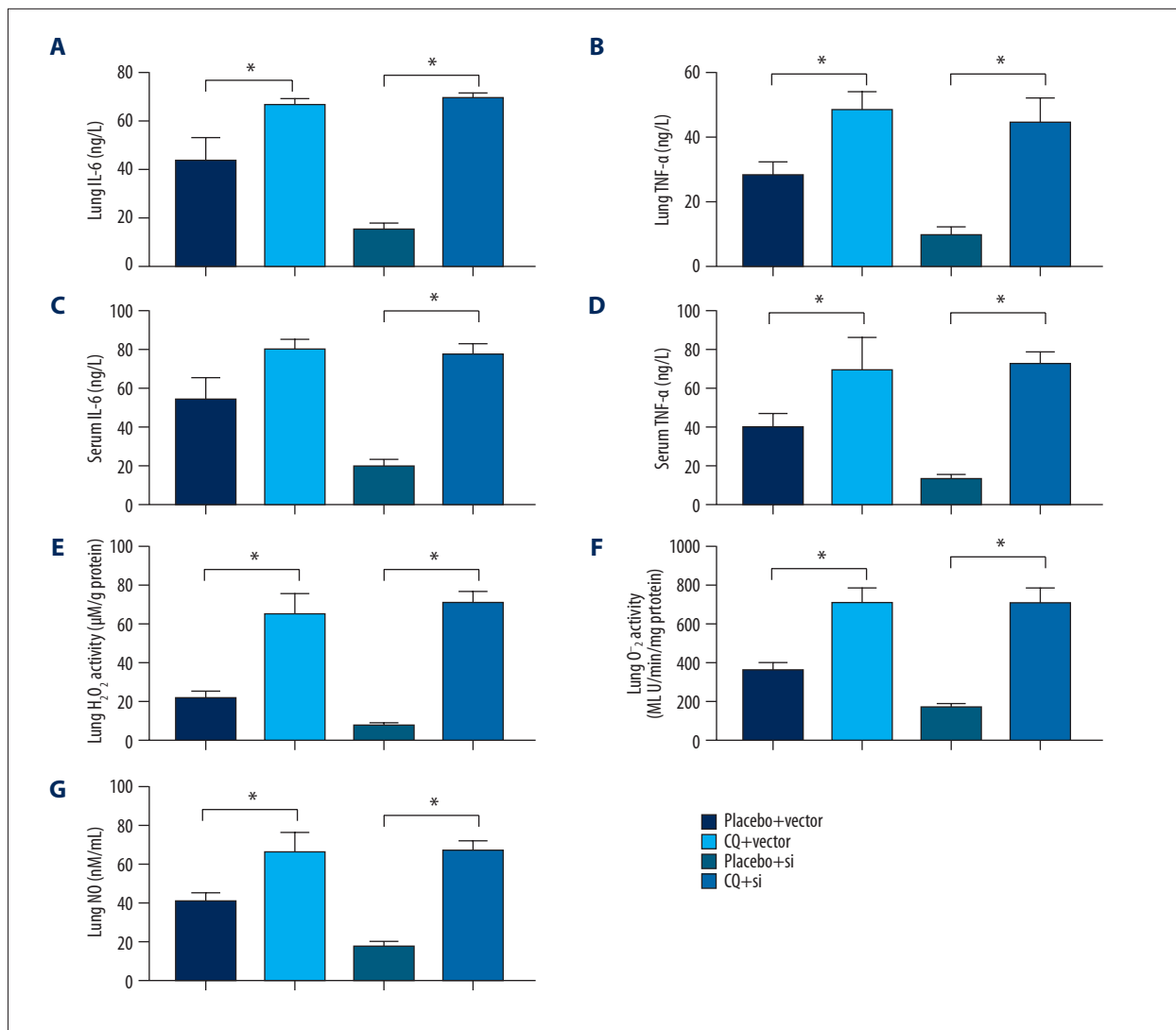


Figure 4. Chloroquine (CQ) reversed the protective effects of HIPK1 interference in LPS-induced ALI mice. (A–D) IL-6 in lung tissues (A) and serum (C), and TNF-alpha in lung tissues (B) and serum (D) of different groups. (E–G) oxidative marker, H₂O₂ (E), O₂⁻ (F), and NO (G) in lung tissues of different groups. The data are presented as means ±SEM (n=3), * p<0.05 compared with the sham group.

ALI mice led to increased autophagic flux and ameliorated inflammation and oxidative stress.

Autophagy consists of several processes: initiation and nucleation, expansion, autophagosome formation, autophagosome-lysosome fusion, and degradation [21]. It has been reported that several markers participate in autophagy, including LC3-II, p62, Atg12-5 complex, Atg3, and Atg7 [11,22–24]. In addition to serving as a marker of autophagy, another important effect of enhanced autophagy activity is increased autophagic flux. The LC3-II accumulation could be the result of increased autophagosome synthesis or decreased degradation; thus, use of overall LC3-II expression may not be appropriate to assess enhanced autophagic flux [25]. Bafilomycin A is a macrolide

antibiotic that inhibits the fusion of autophagosome and lysosome and thus inhibits downstream of LC3-II [25]. As our results showed, bafilomycin A enhanced the expression of LC3-II and HIPK1-interference further enhanced the LC3-II accumulation, thus indicating enhanced autophagic flux after the interference. In addition, we used chloroquine to inhibit the autophagy and assessed whether autophagy is essential in attenuating ALI in HIPK1 interference. The results showed that inhibited autophagy deteriorated the indicators of oxidative stress and inflammation, suggesting the autophagy has an essential role in attenuating ALI in HIPK1 interference.

In the present study, in investigating whether HIPK1 interference protects the lungs via autophagy, we analyzed the

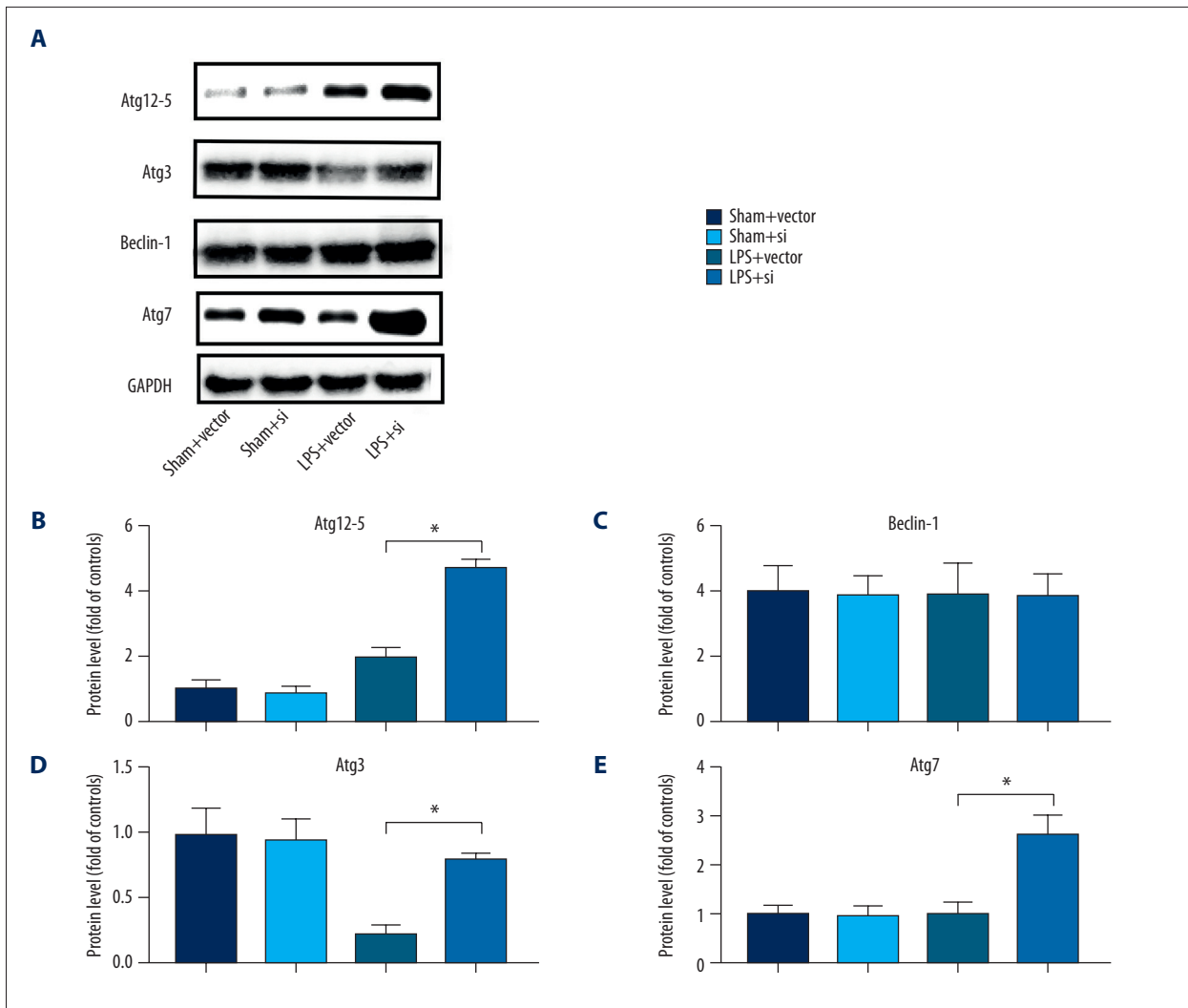


Figure 5. HIPK1 interference enhanced autophagy in LPS-induced ALI mice. (A–E) Western blot (A) and quantification of Atg12-5 (B), Beclin-1 (C), Atg3 (D), and Atg7 (E) in different groups. The data are presented as means \pm SEM (n=3), * $p < 0.05$ compared with the sham group.

expression of autophagic marker and the autophagic flux to prove the elevated autophagy induced by HIPK1 interference. As the results showed, LC3-II was further elevated when compared with the LPS+vector group, and the expression of p62 was decreased. In addition, HIPK1 interference also elevated the expression of Atg12-5 complex, Atg3, and Atg7, indicating enhanced autophagic activity.

In conclusion, HIPK1 interference protected lungs from LPS-induced ALI through autophagy, indicating a promising role as a regulatory target of HIPK1 in future pharmaceutical development. However, further studies are still needed to elucidate

the exact mechanism of HIPK1 interference in regulating autophagy, especially the influence on mTOR signaling.

Conclusions

The present study found that HIPK1 interference ameliorated inflammation and oxidative stress in LPS-induced ALI via enhanced autophagy. These results may provide indications for future pharmaceutical intervention targeted to HIPK1 in the treatment of ALI.

References:

1. Ranieri VM, Rubenfeld GD, Thompson BT et al: Acute respiratory distress syndrome: The Berlin Definition. *JAMA*, 2012; 307: 2526–33
2. Han S, Mallampalli RK: The acute respiratory distress syndrome: From mechanism to translation. *J Immunol*, 2015; 194: 855–60
3. Phua J, Badia JR, Adhikari NK et al: Has mortality from acute respiratory distress syndrome decreased over time?: A systematic review. *Am J Respir Crit Care Med*, 2009; 179: 220–27
4. Zapelini PH, Rezin GT, Cardoso MR et al: Antioxidant treatment reverses mitochondrial dysfunction in a sepsis animal model. *Mitochondrion*, 2008; 8: 211–18
5. Slimen IB, Najar T, Ghram A et al: Reactive oxygen species, heat stress and oxidative-induced mitochondrial damage. A review. *Int j Hyperthermia*, 2014; 30: 513–23
6. Sanchez-Valle V, Chavez-Tapia NC, Uribe M et al: Role of oxidative stress and molecular changes in liver fibrosis: A review. *Curr Med Chem*, 2012; 19: 4850–60
7. Zhang Y, Wang S, Li Y et al: Sophocarpine and matrine inhibit the production of TNF-alpha and IL-6 in murine macrophages and prevent cachexia-related symptoms induced by colon26 adenocarcinoma in mice. *Int Immunopharmacol*, 2008; 8: 1767–72
8. Kundu M, Thompson CB: Macroautophagy versus mitochondrial autophagy: A question of fate? *Cell Death Differ*, 2005; 12: 1484–89
9. Ren C, Zhang H, Wu TT et al: Autophagy: A potential therapeutic target for reversing sepsis-induced immunosuppression. *Front Immunol*, 2017; 8: 1832
10. Jiang Y, Gao M, Wang W et al: Sinomenine hydrochloride protects against polymicrobial sepsis via autophagy. *Int J Mol Sci*, 2015; 16: 2559–73
11. Lin CW, Lo S, Hsu C et al: T-cell autophagy deficiency increases mortality and suppresses immune responses after sepsis. *PLoS One*, 2014; 9, e102066
12. Rey C, Soubeyran I, Mahouche I et al: HIPK1 drives p53 activation to limit colorectal cancer cell growth. *Cell Cycle*, 2013; 12: 1879–91
13. Rinaldo C, Siepi F, Prodosmo A, Soddu S: HIPKs: Jack of all trades in basic nuclear activities. *Biochim Biophys Acta*, 2008; 1783: 2124–29
14. Choi CY, Kim YH, Kim YO et al: Phosphorylation by the DHIPK2 protein kinase modulates the corepressor activity of Groucho. *J Biol Chem*, 2005; 280: 21427–36
15. Kim YH, Choi CY, Lee SJ et al: Homeodomain-interacting protein kinases, a novel family of co-repressors for homeodomain transcription factors. *J Biol Chem*, 1998; 273: 25875–79
16. Nebral K, Denk D, Attarbaschi A et al: Incidence and diversity of PAX5 fusion genes in childhood acute lymphoblastic leukemia. *Leukemia*, 2009; 23: 134–43
17. Sekito A, Koide-Yoshida S, Niki T et al: DJ-1 interacts with HIPK1 and affects H2O2-induced cell death. *Free Rad Res*, 2006; 40: 155–65
18. Kondo S, Lu Y, Debbas M et al: Characterization of cells and gene-targeted mice deficient for the p53-binding kinase homeodomain-interacting protein kinase 1 (HIPK1). *Proc Natl Acad Sci USA*, 2003; 100: 5431–36
19. Poroyko V, Meng F, Meliton A et al: Alterations of lung microbiota in a mouse model of LPS-induced lung injury. *Am J Physiol Lung Cell Mol Physiol*, 2015; 309: L76–83
20. Jin LY, Li CF, Zhu GF et al: Effect of siRNA against NF-kappaB on sepsis-induced acute lung injury in a mouse model. *Mol Med Rep*, 2014; 10: 631–37
21. Kang R, Zeh HJ, Lotze MT et al: The Beclin 1 network regulates autophagy and apoptosis. *Cell Death Differ*, 2011; 18: 571–80
22. Diakopoulos KN, Lesina M, Wörmann S et al: Impaired autophagy induces chronic atrophic pancreatitis in mice via sex- and nutrition-dependent processes. *Gastroenterology*, 2015; 148: 626–38.e17
23. Cutting AS, Del Rosario Y, Mu R et al: The role of autophagy during group B Streptococcus infection of blood-brain barrier endothelium. *J Biol Chem*, 2014; 289: 35711–23
24. Lamoureux F, Thomas C, Crafter C et al: Blocked autophagy using lysosomotropic agents sensitizes resistant prostate tumor cells to the novel Akt inhibitor AZD5363. *Clin Cancer Res*, 2013; 19: 833–44
25. Zhang XJ, Chen S, Huang KX et al: Why should autophagic flux be assessed? *Acta Pharmacol Sin*, 2013; 34: 595–99